Vol. 255: 55–80, 2003 | MARINE ECOLOGY PROGRESS SERIES
Mar Ecol Prog Ser | Published June 24

INTRODUCTION

Marine phytoplankton play a significant role in regulating global atmospheric CO_2 levels (Martin 1990, Cooper et al. 1996). At present, it is not clear how vital algal taxonomic composition is in controlling primary and new production in different oceanic regimes (Falkowski et al. 1998). Recent evidence, however,

nutrient status, or growth rate (e.g. Goericke & Montoya 1998). This approach precludes the importance of nutrient-limited or photoacclimation effects by a population of phytoplankton and assumes that all members of the class will contain the identical pigment ratio. Furthermore, by representing a class of phytoplankton using only 1 pigment or a limited number, the analysis excludes other class members that may not contain the specified pigment (Letelier et al. 1993).

The CHEMTAX (CHEMical TAXonomy) program (a matrix-factorization program for calculating algal abundances from concentrations of algal chemosystematic-marker photopigments) for the MATLAB™ matrix computing system advances our ability to quantify phytoplankton assemblage composition from HPLC-determined pigment concentrations and ratios (Mackey et al. 1996, Wright et al. 1996). It employs a wider suite of pigments and a greater number of phytoplankton classes than previously used. Although the investigator must input an initial pigment ratio for each taxonomic class, the program can alter the pigment ratios, within the bounds set by the investigator, to better match the relative pigment ratios found in the phytoplankton assemblage at a particular locale. This is especially valuable when variations in pigment ratios are expected, for instance, between surface and deeper phytoplankton communities where differences due to photoacclimation may exist, or along transects where latitudinal variations occur.

In 1996 we participated in a cruise on the South

(Fitzwater et al. 1982). Properties measured from the

as well as chl degradation products such as chl-ide, ph-ides, and ph-tin (see Table 1 for list of pigment abbreviations). The system was calibrated by repeated injections of pigment standards that were isolated from a variety of unialgal cultures maintained in the laboratory. Our method could not separate chl *b* and DV chl *b*, so unless otherwise noted the values reported here are for total chl *b* (i.e. the sum of these 2 forms).

Calculation of the relative abundance of various phytoplankton groups from the pigment concentrations was carried out using the CHEMTAX program (Mackey et al. 1996) written for the MATLAB™ matrix computing system. To account for photoacclimation and changes in pigment ratios with depth, samples were divided into depth bins for independent analysis by CHEMTAX. The depth bins used were: 0–10, 10–20, 20–30, 30–50, 50–75, 75–100, and 100–150 m. Samples falling into 2 bins (e.g. a 10 m sample) were included in both bins and the results were averaged. To account for geographical differences in the phytoplankton assemblage, samples were also divided into 2 latitudinal sections. A transition zone between the 2 sections was identified from 44 to 38° S (Stns 86 to 97) across which the depth of the 1% isolume increased from 60 to 100 m. South of the transition zone surface DV chl *a* concentration was 0, increasing to 30 ng l^{-1} within the transition zone and decreasing slightly fur-

Table 3. General distribution pattern of various physical, chemical and biological core parameters in regimes of South Pacific Ocean during January to March 1996. Values for core parameters represent values measured within mixed layer for each specific region (mean ± SD). Dominant algal groups were determined using CHEMTAX analysis of HPLC pigment data. Abbreviations as in Table 1

Zone	Latitude (°S)	Station #	*T* (°C)	Salinity (psu)	Total chl *a* (ng l^{-1})	NO_3 (µM)	PO_4 (µM)	SiO_4 (µM)	Dominant algae

to identify the regions and oceanic fronts crossed along the transect (Daly et al. 2001). Temperature stratification occurred in the STF (45 to 40°S) at 30 to 50 m (Fig. 2A) and deepened northward into the SPG. The average temperature increased northward across the frontal zones and into the SPG; it reached a maximum in the SPG and decreased slightly in the EZ, presumably due to upwelling (Fig. 2A). Little vertical structure in salinity distributions occurred in the upper 150 m, except in the central part of the SPG (Fig. 2B). The average salinity increased northward across the fronts and into the southern part of the SPG (Table 3), decreased in the central axis region due to precipitation (Hansell & Feely 2000), but increased again upon entering the EZ (Fig. 2B).

Both nitrate and phosphate concentrations decreased northward across the fronts and into the SPG, dropping to below detectable levels (<0.1 µM) in the SPG (Fig. 3A,B, Table 3). Concentrations of both nutrients rose slightly in the EZ. Silicate concentrations were highest (>60 µM) at the southernmost (ca. 67°S) station (#33), and decreased markedly across the SF (Fig. 3C, Table 3). Low silicate concentrations (<1 µM) were measured north of the STF. Ammonium concentrations were greatest (ca. 1 µM) between 70 and 100 m in the SF, SAF, and STF (Fig. 3D). In the SPG, NH_4^+ levels were typically undetectable (<0.1 µM), but slightly greater concentrations were found in the EZ. Urea concentrations were typically at or below our detection limits (<0.1 µM) and did not reveal any significant relationships with depth or oceanographic province (data not shown).

Pigment concentrations

The SAF generally contained lower pigment concentrations than the zones and fronts to the north or south. Surface chl *a* concentrations in the SAF were only 27 and 36% of the concentrations in the PF and STF (Table 3), and depth-integrated chl *a* was 30 and 42%, respectively (Table 4). In the STF, at about the depth of the 1% isolume (45 m), we observed a subsurface chlorophyll maximum (SCM), deepening northward to about 120 m between 20 and 10° S (Fig. 4A). The SCM dissipated near the Equator. Chl *a* concentrations exceeded 500 ng l^{-1} in the PF and STF, while elsewhere concentrations rarely exceeded 300 ng l^{-1}. In the southern part of the SPG, chl *a* concentrations in the SCM were much greater

with lower values south of the SAZ (Table 4). Total chl *b* concentrations were always greatest in the SCM, and across the SPG concentrations in the SCM were ≥100 ng l^{-1}. In the SPG north of 32° S, there was more total chl *b* below 100 m than above (Table 5). In the EZ, there was more total chl *b* above 100 m than deeper. chl c_1+c_2 concentrations were greatest within and south of the PF, with lesser amounts in the STF and minor amounts in the SCM of the SPG (Fig. 4C). Depth-integrated amounts of chl c_1+c_2 varied only from 1.1 to 4.6 mg m^{-2} across the entire transect (Table 4). Chl c_3

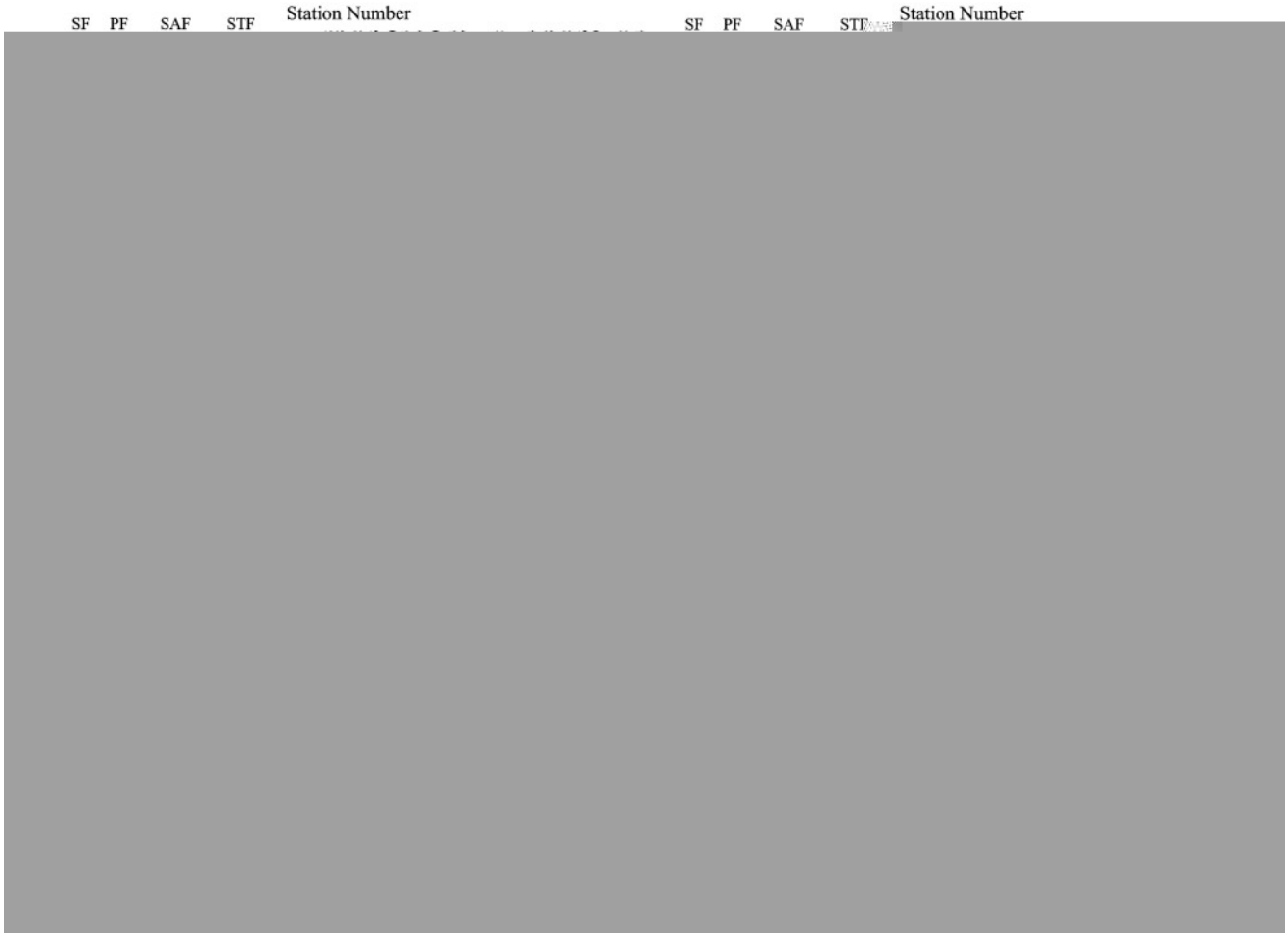

Fig. 5. Major carotenoid concentration profiles (ng l^{-1}) along sampling transect: (A) 19'-butanoyloxyfucoxanthin; (B) fucoxanthin; (C) 19'-hexanoyloxyfucoxanthin; (D) zeaxanthin

Low concentrations of DV chl *a*, found only in *Pro* (Chisholm et al. 1988, Goericke & Repeta 1992), were measured in the STF (Table 4), but only at depth (see Fig. 13D). While maximum DV chl *a* concentrations were found in the SCM of the SPG (with values exceeding 80 ng l^{-1} across the entire region) the depth-integrated values of DV chl *a* showed approximately equal amounts above and below 100 m (Table 5). In contrast, the maximum DV chl *a* concentrations in the EZ was observed in the upper 100 m (see Fig. 13D), resulting in 5-fold higher DV chl *a* concentrations in the upper 100 m than below (Table 5). In the SPG, the DV chl *a*:total chl *a* ratio was ca. 0.45 in both the upper (0 to 100 m) and lower (101 to 150 m) photic zones. In the EZ, the ratio in the upper photic zone was similar (0.44) to that in the SPG, but was only 0.29 in the lower photic zone. The DV chl *a*:total chl *b* ratio in the upper photic zone was greatest in the central and northern part of the SPG, and lower in the southern part of the SPG and in the EZ (Table 5). A lower DV chl *a*:total chl *b* ratio was observed below 100 m in both the SPG and EZ, similar to laboratory results with *Pro* demonstrating a decrease in this ratio at lowered growth irradiances (Partensky et al. 1993).

Distributions of 3 of the 4 major carotenoids found in these waters, 19but, Fucox, and 19hex, followed a pattern similar to that of the chlorophylls (Fig. 5A–C). Highest concentrations were generally observed in the SF, PF, and STF with a band of elevated concentrations in the SCM across the SPG. The concentration of 19but was greatest in the PF and the STF, exceeding 120 ng l^{-1}. In the SPG, 19but concentrations were greatest in the SCM layer, with low concentrations north of 30° S, primarily in the SCM. There were slightly elevated concentrations (up to 50 ng l^{-1}) of 19but in the EZ. Depth-integrated (0 to 150 m) amounts of 19but were remarkably uniform across the entire transect (Table 4). Fucox concentrations were greatest south of the PF, exceeding 200 ng l^{-1} in some samples. Lower concentrations of Fucox were found in the PF and the SAF

(<100 ng l^{-1}), with little or none found further north in

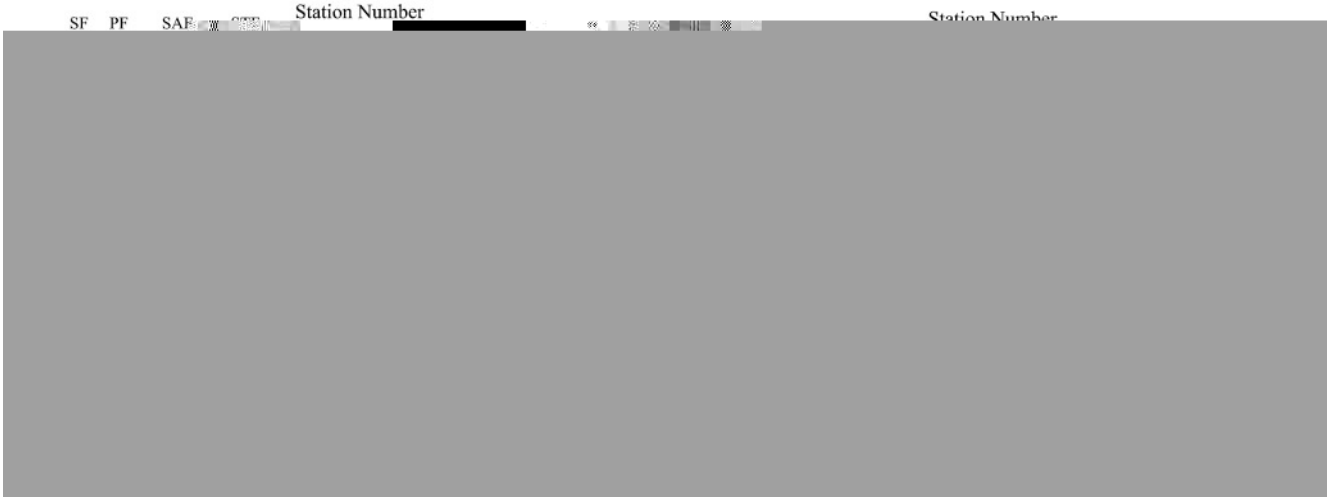

Fig. 7. Productivity along sampling transect. (A) Primary production measured by ^{13}C incorporation (ng C l^{-1} h^{-1}); (B) productivity index (g C g^{-1} chl *a* h^{-1})

Flow cytometry

Samples for flow cytometry were collected only from Stns 116 (34° S) to 174 (Equator) and counted to determine the abundance of *Syn*, *Pro*, heterotrophic bacteria, and pico-eukaryotic algae (Fig. 8). In the euphotic zone, heterotrophic bacteria were always the most abundant cell type, and were relatively uniform along the transect, ranging between 5×10^5 to 7×10^5 cells ml^{-1} (data not shown), and decreasing below the euphotic zone. *Pro* were the next most abundant group (Fig. 8B) with cell densities ranging up to 2.9×10^5 cells ml^{-1}. *Syn* (Fig. 8A) were more abundant than pico-eukaryotes (Fig. 8C), except at the surface in the EZ, where they were approximately equal. Prokaryotic cells were always greater in surface waters (<50 m) than at depth; however, the latitudinal distribution varied by group. The highest *Syn* cell counts were measured in the EZ, while *Pro* cell counts were highest in the SPG (20 to 25° S). Depth-integrated *Pro* cell counts were 22 and 51% lower in the EZ relative to the SPG above and below 100 m, respectively (Table 5). In conjunction with this decrease in *Pro* abundance, depth-integrated *Syn* cell counts increased by 457 and 267% in the EZ relative to the SPG above and below 100 m, respectively (Table 4). Pico-eukaryotic cell counts were greatest in the surface waters of the EZ, but in the SPG cell counts were slightly greater in the SCM than at the surface.

The ratio of DV chl *a*:*Pro* cell number increased at depth, especially below the depth of 1% surface irradiance, suggesting that photoacclimation was significant (Fig. 8D). In the SPG, the ratio of DV chl *a* per cell in the upper 100 m averaged 0.14 fg $cell^{-1}$, whereas the ratio between the 1% light level (ca. 100 m) and 0.1% light level (ca. 150 m) was nearly 10-fold higher (Table 5). Ratios exceeding 4 fg DV chl *a* $cell^{-1}$ were observed between 200 and 250 m (data not shown).

CHEMTAX

The results of the CHEMTAX analyses are presented in 2 ways: as a percentage of the total chl *a* contained in each taxonomic group, and as the amount of chl *a* or DV chl *a* contained in each group (Figs. 9 to 13). The first analysis shows the relative contribution of a group to the phytoplankton assemblage at a given location, whereas the second analysis shows the relative biomass distribution of a group along the transect. As previously described, a transition zone existed between 44 and 38° S (Stns 86 to 97), across which the depth of the 1% isolume increased from 60 to 100 m. South of this zone the dominant taxonomic groups were diatoms (Fig. 9A,B),

Table 6. Zonal differences in areal rates of primary production (integrated to depth of euphotic zone) and surface productivity index. N = no. of samples

Zone	Station #	N	Primary productivity (g C m^{-2} d^{-1})	Surface productivity index (g C [g total chl *a*]$^{-1}$ h^{-1})
AZ	33–47	3	0.32 ± 0.10	2.78 ± 2.28
STZ	62–76	3	0.76 ± 0.05	3.59 ± 1.67
SPG	101–162	8	0.58 ± 0.44	5.68 ± 2.60
EZ	169–172	2	2.43 ± 0.23	8.32 ± 5.23

surface phytoplankton assemblage south of the PF, with a secondary peak at 90 m in the PF (Fig. 11C,D).

Chlorophytes were negligible members of the phytoplankton assemblage, always containing less than 5% of the total chl *a* and rarely more than 10 ng chl *a* l^{-1}

(Mitchell & Holm-Hansen 1991). Mengelt et al. (2001) also concluded that by summer, light-limitation no longer limits phytoplankton growth in this region. Therefore, we would expect to observe higher biomass and productivity at Stn 33 than north of the SF. However, while Stn 33 contained only moderate algal biomass levels (chl *a* <300 ng l^{-1}) and low rates of PP (<400 ng C l^{-1} h^{-1}) at the surface, stations north of the SF had both high biomass (chl *a* > 500 ng l^{-1}) and PP rates (>1000 ng C l^{-1} h^{-1}). In addition to possible light limitation, iron is probably a major factor limiting PP and biomass south of the SF (Martin et al. 1990, Boyd et al. 1995,1999, Franck et al. 2000, Mengelt et al. 2001), particularly during austral summer. The *in situ* correlation of dissolved iron and algal biomass distribution in the Southern Ocean supports the iron-limitation hypothesis (de Baar et al. 1995, Boyd et al. 1999, 2000, Sedwick et al. 1999, Franck et al. 2000, Mengelt et al. 2001). In the Pacific sector of the Southern Ocean Nolting et al. (1998) and van Leeuwe et al. (1998b) found lower iron concentrations in the water masses of the AZ than further north, and that the iron that is present may not be

Antarctic circumpolar current

The SF and PF are important zones for biological production (Selph et al. 2001). These zones accumulate suspended particulate matter (Bidigare et al. 1996, Nelson et al. 1996, Moore et al. 1999) and the vertical stability maintains a favorable light environment for phytoplankton growth. Stratification was observed at moderate depths (60 to 80 m) between the SF and the PF, and only slightly deeper (about 45 m) than the euphotic zone (Daly et al. 2001). Advection of nutrients into the SF by upwelling maintains high iron and nutrient concentrations favorable for growth (Löscher 1999, Mengelt et al. 2001), but the sinking of biogenic particles rich in silicate will balance this input over seasonal and annual timescales. During the summer, grazing by mesozooplankton can consume up to 21% of the daily phytoplankton production (Urban-Rich et al. 2001). While total chl *a* was about the same in the PF as further south, a series of cloudy days with slightly lower irradiance levels (average PAR of 501 ± 221 µE m^{-2} s^{-1} from 63 to 50° S) resulted in a lower PP than in the AZ.

Fig. 12. CHEMTAX analysis results. (A) % total chl *a* in chlorophytes; (B) chl *a* concentration (ng l^{-1}) in chlorophytes; (C) % total chl *a* in prasinophytes; (D) chl *a* concentration (ng l^{-1}) in prasinophytes

ble for the drawdown in silicate concentrations in spring and summer (Hutchins et al. 2001). North of the PF, pelagophytes, Hapto3, and Hapto4 cells continued to increase in biomass and dominance, with a decline in the dominance of diatoms, most probably due to the co-limitation of iron and silicate on diatom growth, especially in the mid- to late-summer period (Nelson & Tréguer 1992, van Leeuwe et al. 1998b, Boyd et al. 1999, de Baar et al. 1999). However, diatoms still represented 10 to 30% of the total chl *a* in the low-silicate waters between 60 and 55° S. The low concentrations of silicate and the lower abundance of diatoms observed in this region may have resulted from a spring diatom bloom that subsequently sank or was effectively grazed from the surface waters. Within transects across the PF during austral spring (October and November), several studies (Boyd et al. 1995, Peeken 1997, Smith et al. 2000, Nelson et al. 2001) found high silicate concentrations and phytoplankton assemblages dominated by diatoms. Transects conducted across the PF during summer and fall (January to May) typically find few diatoms and low silicate concentrations (Sullivan et al. 1993, van Leeuwe et al. 1998a, de Baar et al. 1999, Smith et al. 2000, Brown & Landry 2001). During the seasonal progression north of the PF, iron and silicate are probably co-limiting nutrients (Franck et al. 2000). Following the initial diatom bloom, low iron availability can result in enhanced silicate:nitrate uptake ratios for pennate diatoms, leading to a population of thickly silicified cells (Hutchins & Bruland 1998, Takeda 1998, Franck et al. 2000) and a rapid drawdown of silicate concentrations. Even in low-silicate subantarctic waters near Tasmania, lightly silicified pennate diatoms have been observed to proliferate in bottle incubations following iron-addition (Sedwick et al. 1999, Hutchins et al. 2001). Hence, seasonal iron depletion could result in dominance by thickly silicified diatom species during the spring bloom, a transi-

Fig. 13. CHEMTAX analysis results. (A) % total chl *a* in *Synechococcus* spp.; (B) chl *a* concentration (ng l^{-1}) in *Synechococcus* spp.; (C) % total chl *a* in *Prochlorococcus* spp.; (D) divinyl chl *a* concentration (ng l^{-1}) in *Prochlorococcus* spp.

tion to lightly silicified diatoms as silicate becomes limiting, and finally to flagellates when silicate is exhausted during the summer. Other nutrients (nitrate, phosphate, trace metals, etc.) are more rapidly and efficiently recycled by zooplankton grazing (Daly et al. 2001), and are thus not as greatly diminished by the particulate sinking flux.

The distribution of Σph-ide revealed that the most significant processes producing phaeopigments were associated primarily with the region south of the SAF, where the phytoplankton assemblage was dominated by diatoms. Because a mixture of both 'normal' phaeophorbide *a* and pyrophaeophorbide *a* was observed in this region, it is likely that both grazing and senescent processes produced these. Via enhanced settling rates and lowered losses due to mesozooplanktonic grazers and recycling processes, it is possible that diatoms increase the efficiency of the biological pump (Dugdale et al. 1995) compared to smaller phytoplankton species. However, this may not entirely be the case when iron and silicate are severely co-limiting diatom growth. Under iron limitation, cell size is reduced (Sunda & Huntsman 1997) and smaller diatom species tend to dominate the phytoplankton assemblage (Hutchins et al. 2002). These smaller diatom species may be more susceptible to mesozooplanktonic grazing, which may explain the Σph-ide maximum observed south of the SAF (Fig. 6). Jónasdóttir et al. (1998) suggested that some diatoms inhibit grazing via chemical defense mechanisms, although the effect of individual species on copepod growth and reproduction is poorly known. Ingestion of diatoms by grazers is probably a complex function of species, size, and chemical composition, and our data cannot discern the dominant effect in this region.

The SAF is a region of lower pigment concentrations between the PF and the STF, typical of an HNLC area described by Minas & Minas (1992). Surface geo-

strophic velocities were maximal at the SAF (Daly et al. 2001); this increased the depth of the surface mixed layer to 80 to 100 m, i.e. below the 1% isolume at 60 m. It is conceivable that light limitation could have accounted for the observed low biomass (Mitchell & Holm-Hansen 1991). Hapto3 and pelagophytes dominated the surface phytoplankton assemblage, both in terms of abundance and biomass, even as chl *a* decreased (from >200 to <50 ng l^{-1}) between the PF and the SAF. The abundance and biomass of diatoms decreased sharply along with the decline in silicate concentrations until they accounted for <10% of the total chl *a*. Conversely, the abundance and biomass of the minor components of the assemblage (cryptophytes, chlorophytes, and prasinophytes) continued to increase to the north. For the first time on the transect we observed a SCM at the depth of strong stratification. Pigment concentrations were greater at depths between 30 and 100 m than at the surface, and most groups showed greater chl *a* biomass at these depths than at the surface. Hapto4 cells dominated the phytoplankton assemblage in the SCM.

While blooms of colonial *Phaeocystis antarctica* are

comprised a minor portion of the assemblage (< 30 %). *Pro* dominated the surface assemblage both in terms of total chl *a* biomass and numerically, based on the flow cytometry results, while *Syn* ranked second. In contrast, Mackey et al. (1998), using CHEMTAX to analyze the pigment distribution in the western tropical Pacific, concluded that *Syn* dominated the chl biomass in surface waters and *Pro* was of secondary importance. In the same region, Shimada et al. (1993) reported that *dominated the chl biomass in sur-*

Equatorial Zone

North of 10° S the cruise entered the EZ, a region of equatorial upwelling with hydrographic conditions consistent with non-El Niño periods (Ishizaka et al. 1997). In fact, this cruise took place at the beginning of a La Niña event (Le Borgne et al. 1999). This HNLC regime is distinct from both the SPG and the oligotrophic warm pool of the western Equatorial Pacific (Blanchot et al. 2001) by having a shallow and dispersed SCM, elevated macronutrient (NO_3^-, PO_4^-, NH_4^+) concentrations, a shallower euphotic zone, and slightly higher pigment concentrations. Consistent with other reports (Iriarte & Fryxell 1995, Raimbault et al. 1999, Blanchot et al. 2001), a surface mixed layer of 60 to 90 m depth, slightly shallower than the euphotic zone, is generally distinguished from deeper waters and contains the majority of the phytoplankton cell numbers and biomass (Chavez et al. 1990, Le Bouteiller et al. 1992, Kaczmarska & Fryxell 1995, André et al. 1999, Blanchot et al. 2001). In this region, surface ^{13}C PP was comparable to values observed in the STF, where nutrient concentrations were similar but not as great as would be expected in a tropical environment. Our average surface productivity indices (8 g C [g total chl *a*]$^{-1}$ h^{-1}) in the EZ were similar to those measured (photosynthesis–irradiance [P–I] values of 5 to 6) in February and March, 1988 along 150° W (Cullen et al. 1992). Our P–I values, however, were significantly lower than those measured in other warm waters (>26°C) with re-

plankton assemblage between ecosystems. Because CHEMTAX calculates a single final pigment ratio matrix for the entire data set being analyzed, the analysis of a large set of samples must have the sample set broken up into discrete sets based on environmental parameters for separate analyses. Expecting variations in the pigment ratios within each algal group due to photoacclimation and taxonomic changes between ecosystems, we chose to divide our large sample set (270 samples) into 7 depth bins and 2 latitudinal sections for 14 separate analyses. There is no need, however, for the user to absolutely define the pigment-ratio matrix for each analysis beforehand. Instead, CHEMTAX allows the user-defined initial pigment-ratio matrix to shift during the analysis based on a continual comparison of the pigment-ratio matrix to the data set. This allows the user some latitude in defining the initial pigment-ratio matrix. While it is best for the user to create the most accurate initial pigment-ratio matrix possible in order to calculate the phytoplankton assemblage composition, CHEMTAX is tolerant of random variations in the initial pigment ratio matrix as well as in the pigment-data matrix (Mackey et al. 1997). Subtle variations in pigment ratios due to light, nutrient, or other environmental parameters have only a minor impact on the CHEMTAX biomass calculations (Schlüter et al. 2000), and CHEMTAX analyses of pigment concentrations often have high correlations with microscopic enumeration (Lampert et al. 2000). At very low pigment concentrations, where small inaccuracies in determining the pigment concentrations can result in significantly large changes in pigment ratios, CHEMTAX has problems distinguishing between algal groups with similar suites of pigments (e.g. Hapto3 and Hapto4). In our analyses this was especially apparent in samples collected from deep waters (>150 m) and from the surface waters of the SPG. This problem can be partially offset by more accurately defining the initial pigment-ratio matrix.

CONCLUSIONS

Our results documented the large-scale distributional patterns of phytoplankton biomass, assemblage composition, and productivity in the South Pacific Ocean. Differences in both algal abundance and productivity rates were not unexpected, given the wide range in environmental factors that control and influence both. Such environmental variables also are expected to change over time, and the associated biogeochemical processes will undoubtedly be altered. Knowledge of the broad basin-wide pattern of phytoplankton distribution is a first step in the assessment of these long-term trends.

Acknowledgements. We appreciate the efforts of the captain and crew of the NOAA RV 'Discoverer'. We thank Drs. G. Johnson for the hydrographic data, C. Mordy for the nitrate, phosphate and silicate analyses, and Francisco Chavez for use of the irradiance data. Funding for this research was provided by an NOAA-Program of Global Climate Change grant to G.R.D. and W.O.S. as well as NSF-OCE grants to G.R.D. (9504382) and L.C. (9696198). Additional funding for the she captaiirst stp 3 c9lankton bi/e captaioosp Tc9ue.ch enviTacaptain

Southern Ocean stimulated by iron fertilization. Nature 407:695–702

Boyd PW, Newton (1999) Does planktonic community structure determine downward particulate organic carbon flux in different oceanic provinces? Deep-Sea Res 46:63–92

Boyd PW, Robinson C, Savidge G, Williams PJ, Le B (1995) Water column and sea-ice primary production during Austral spring in the Bellinghausen Sea. Deep-Sea Res II 42: 1177–1200

Bradford-Grieve JM, Chang FH, Gall M, Pickmere S, Richards F (1997) Size-fractioned phytoplankton standing stocks and primary production during austral winter and spring 1993 in the Subtropical Convergence region near New Zealand. NZ J Mar Freshw Res 31:201–224

Brown SL, Landry MR (2001) Microbial community structure and biomass in surface waters during a Polar Front summer bloom along 170° W. Deep-Sea Res II 48:4039–4058

Campbell L, Vaulot D (1993) Photosynthetic picoplankton community structure in the subtropical North Pacific ocean near Hawaii (Station ALOHA). Deep-Sea Res 40: 2043–2060

Campbell L, Nolla HA, Vaulot D (1994) The importance of *Prochlorococcus* to community structure in the central North Pacific Ocean. Limnol Oceanogr 39:954–961

Chang FH, Gall M (1998) Phytoplankton assemblages and photosynthetic pigments during winter and spring in the Subtropical Convergence region near New Zealand. NZ J Mar Freshw Res 32:515–530

Chavez FP, Buck KR, Barber RT (1990) Phytoplankton taxa in relation to primary production in the equatorial Pacific. Deep-Sea Res 37:1733–1752

Chisholm SW, Olson RJ, Zettler ER, Goericke R, Waterbury

Higgins HW, Mackey DJ (2000) Algal class abundances, estimated from chlorophyll and carotenoid pigments, in the western Equatorial pacific under El Niño and non-El Niño conditions. Deep-Sea Res I 47:1461–1483

Mitchell BG, Holm-Hansen O (1991) Observations and modeling of the Antarctic phytoplankton crop in relation to mixing depth. Deep-Sea Res 38:981–1008

Mitchell GB, Brody E, Holm-Hansen O, McClain CR, Bishop J (1991) Light limitation of phytoplankton biomass and macronutrient utilization in the Southern Ocean. Limnol Oceanogr 36:1662–1677

Moon-van der Staay SY, van der Staay GWM, Guillou L, Vaulot D, Claustre H, Medlin LK (2000) Abundance and diversity of prymnisiophytes in the picoplankton community from the equatorial Pacific Ocean inferred from 18S rDNA sequences. Limnol Oceanogr 45:98–109

Moore JK, Abbott MR, Richman JG (1999) Location and dynamics of the Antarctic Polar Front form satellite sea surface temperature data. J Geophys Res 104:3059–3073

Moore LR, Rocap G, Chisholm SW (1998) Physiology and molecular phylogeny of coexisting *Prochlorococcus* ecotypes. Nature 393:464–467

Mulvenna PF, Savidge G (1992) A modified manual method for the determination of urea in seawater using diacetylmonoxime reagent. Estuar Coast Shelf Sci 34:429–438

Nelson DM, Smith WO Jr (1991) Sverdrup revisited: critical depths, maximum chlorophyll levels and the control of Southern Ocean productivity by the irradiance/mixing regime. Limnol Oceanogr 36:1650–1661

Nelson DM, Tréguer P (1992) Role of silicon as a limiting nutrient to Antarctic diatoms: evidence from kinetic studies in the Ross Sea ice-edge zone. Mar Ecol Prog Ser 80: 255–264

Nelson DM, DeMaster DJ, Dunbar RB, Smith WO Jr (1996) Cycling of organic carbon and biogenic silica in the Southern Ocean: estimates of water-column and sedimentary fluxes on the Ross Sea continental shelf. J Geophys Res 101:18519–18532

Nelson DM, Brzezinski MA, Sigmon DE, Franck VM (2001) A seasonal progression of Si limitation in the Pacific sector of the Southern Ocean. Deep-Sea Res II 48:3973–3995

Nodder S, Gall M (1998) Pigment fluxes from the Subtropical Convergence region, east of New Zealand: relationships to planktonic community structure. NZ J Mar Freshw Res 32:441–465

Nolting RF, Gerringa LJA, Swagerman MJW, Timmermans KR, de Baar HJW (1998) Fe (III) speciation in the high nutrient, low chlorophyll Pacific region of the Southern Ocean. Mar Chem 62:335–352

Olson RJ, Chisholm SW, Zettler ER, Armbrust EV (1988) Analysis of *Synechococcus* pigment types in the sea using single and dual beam flow cytometry. Deep-Sea Res 35: 425–440

Olson RJ, Chisholm SW, Zettler ER, Altabet MA, Dusenberry JA (1990) Spatial and temporal distributions of prochlorophyte picoplankton in the North Atlantic Ocean. Deep-Sea Res 37:1033–1051

Olson RJ, Sosik HM, Chekalyuk AM, Shalapyonok A (2000) Effects of iron enrichment on phytoplankton in the Southern Ocean during late summer: active fluorescence and flow cytometric analyses. Deep-Sea Res II 47:3181–3200

Orsi AH, Whitworth T III, Nowlin WD Jr (1995) On the meridional extent and fronts of the Antarctic Circumpolar Current. Deep-Sea Res I 42:641–673

Parsons TR, Maita Y, Lalli CM (1984) A manual of chemical and biological methods for seawater analysis. Pergamon Press, New York